Fachtagung "Experimentelle Strömungsmechanik"
7. – 9. September 2021, Bremen

A model for the determination of vehicle-induced aerodynamic lateral loads on cyclist during overtaking maneuvers

Ein Modell zur Bestimmung von verkehrsinduzierten aerodynamischen Seitenkräften auf Fahrradfahrer während Überholvorgängen

Christof Gromke[1,*], Bodo Ruck[1]
[1]Karlsruhe Institute of Technology KIT, Institute for Hydromechanics, Laboratory of Building and Environmental Aerodynamics, Karlsruhe, Germany
[*]gromke@kit.edu

Key words: overtaking maneuver, vehicle-induced load, cyclist lateral load
Schlagworte: Überholmanöver, Fahrzeug-induzierte Kraft, Seitenlast auf Fahrradfahrer

Abstract

In a comprehensive field measurement campaign vehicle-induced lateral loads acting on cyclists during overtaking maneuvers were acquired. The study comprised five vehicle types - a station wagon as a representative for the type passenger car, a 3.5 t van, a 7.5 t truck, a 40 t semitrailer truck, and a tour bus - in combination with four types of cyclists - an adult person on a touring bike with and without saddle bags, an adult person on a racing bike, and an adolescent person on a juvenile bike - being represented by corresponding life-size dummies. Time histories of the lateral load were acquired for overtaking maneuvers of different velocities ranging from 30 to 100 km h^{-1} and of different overtaking distances ranging from 0.5 to 2.0 m.
Common to the time histories of all combinations of vehicle and cyclist types is a steady increase in the lateral load while the vehicle is approaching the cyclist from the back. At this stage, the overtaking vehicle exerts a pressure load which acts to push the cyclist away from it towards the curbside. When the vehicle is next to the cyclist, the magnitude of the load rapidly falls off, changes direction, and the vehicle exerts a suction load which acts to draw the cyclists towards the vehicle. This change in load direction is considered critical for cyclist safety since it happens rather suddenly and very quickly - typically in a time span of 0.1 to 0.2 seconds - and may provoke a reflexive compensatory steering maneuver whereby the rider loses control.
Based on the measurement data and curve fitting, a mathematical model was established which allows to calculate the maximum and minimum loads, i.e. the peak pressure and peak suction load laterally acting on the various cyclist types when being overtaken by a certain type of vehicle.

Introduction

Road vehicles exert unsteady aerodynamic loads on cyclists during overtaking maneuvers. The aerodynamic loads thereby show components in and perpendicular to the driving direction. Depending on the stage of the overtaking maneuver, the perpendicular load component acts either in the direction towards the cyclist or in the direction towards the vehicle (Gromke and Ruck 2019a, 2019b, 2021). This load, and in particular the change of load direction, is perceived as a disturbance by the cyclist and may trigger a compensatory reaction with the aim to adjust to the changed equilibrium condition and to restore balance. However, if the disturbance is too strong and / or too sudden and quick, the cyclist may not be able to appropriately react and, as a consequence, may lose control and finally tumble or collide with the overtaking vehicle or other objects.

Measurement Series

Lateral loads on various life-size person dummies on different bike types during overtaking maneuvers by several vehicle types were acquired in field measurements (Fig. 1). The dummy-bike assemblies were attached to a fixed rack by means of 4 truss members with uniaxial S-beam load cells at their ends which measured the horizontal load transfered at the center of the top tube and the tire contact points. Overtaking maneuvers were performed with different vehicle types (Fig. 1) by variation of vehicle speed V_{veh} (nominal: 30, 40, 50, 60, 70, 80, 90, and 100 km h^{-1} depending on vehicle type) and overtaking distance d_y (nominal: 0.5, 1.0, 1.5, and 2.0 m), where d_y is defined as the spacing between the car envelope - excluding the protruding side mirror - and the central vertical plane of the dummy-bike assembly defined by the bicycle frame. Each combination of overtaking speed and distance was carried out four to five times and the data were ensemble-averaged. The actual vehicle speed and overtaking distance were acquired by the cruise control of the car and an electro-optic distance sensor.

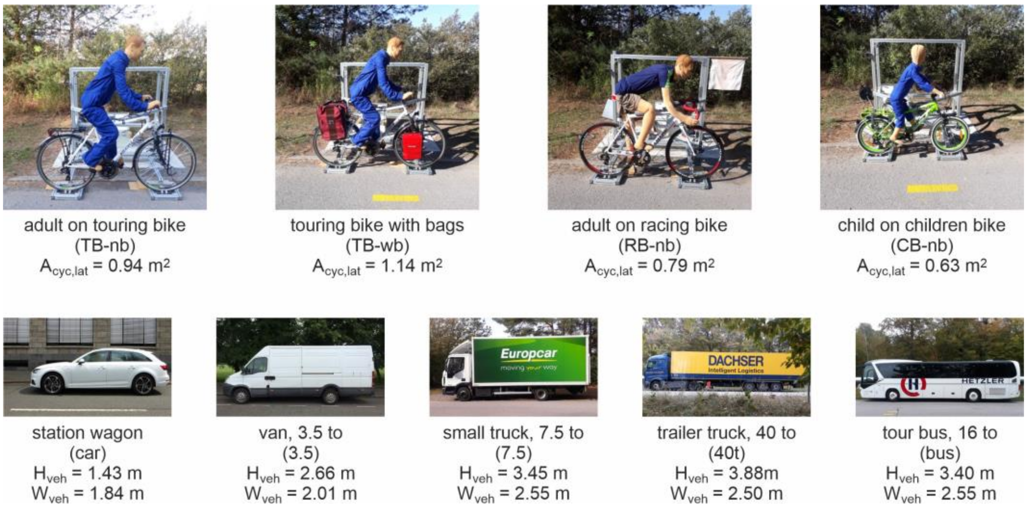

Fig. 1: Overview of cyclist types and vehicle types. The terms in brackets indicate the abbreviations utilized hereinafter to identify cyclist and vehicle type ($A_{cyc,lat}$: cyclist lateral area, H_{veh}: vehicle height, W_{veh}: vehicle width).

Results and Discussion

Fig. 2 shows by way of example the load time history acquired in an overtaking maneuver of the adult dummy on the touring bike without saddle bags (TB-nb) by the station wagon. The following 5 distinctive phases in the time history can be identified:

GALA e.V., Karlsruhe, Germany, ISBN 978-3-9816764-7-1

- P-1: A phase with an increasing pressure load which acts to push the cyclist away from the vehicle while it is approaching.
- P-2: A phase with a relatively sudden and rapid flip over from pressure to suction load.
- P-3: A phase with a predominant suction load which acts to pull the cyclist towards the overtaking vehicle.
- P-4: A phase with a second (reverse) flip over from suction to pressure.
- P-5: A final phase in which the load declines to zero superimposed by decaying oscillation-like fluctuations when the vehicle has overtaken the cyclist.

As argued before, the phase with the relatively rapid flip over from pressure to suction load (P-2) is considered in particular critical for cyclist safety. For this reason, the peak pressure load and the peak suction load marking the onset and the end of phase P-2 are examined in more detail in the reminder of this contribution.

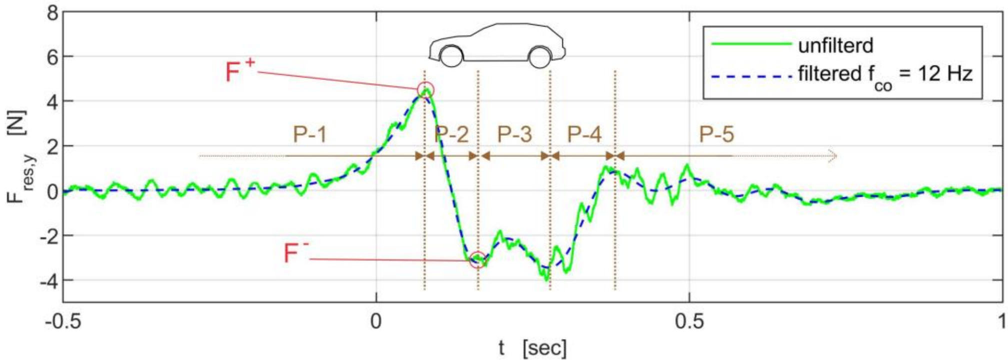

Fig. 2: Load time history obtained in an overtaking maneuver of the touring bike cyclist (TB-nb) by the station wagon (V_{veh} = 80 km h^{-1}, d_y = 1.0 m).

Peak pressure load

Peak pressure loads F^+ in dependency on vehicle speed and overtaking distance are presented in Fig. 3 for selected combinations of cyclist-vehicle types. The symbols indicate measured values and the dashed lines curve fits are obtained by a quadratic relation according to

$$F^+ = c_1 V_{veh}^2 \qquad (1)$$

where V_{veh} is the vehicle speed [m s^{-1}] and c_1 a pre-factor [kg m^{-1}] pertaining to a cyclist-vehicle type combination at overtaking distance d_y. The choice of a quadratic relation was motivated by the well-established relation for turbulent flows where the fluid dynamical load scales with the square of the fluid velocity, which, in turn, is assumed to scale linearly with vehicle speed and is, a posteriori, substantiated by the large values of the coefficient of determination (R^2 > 0.85 always).

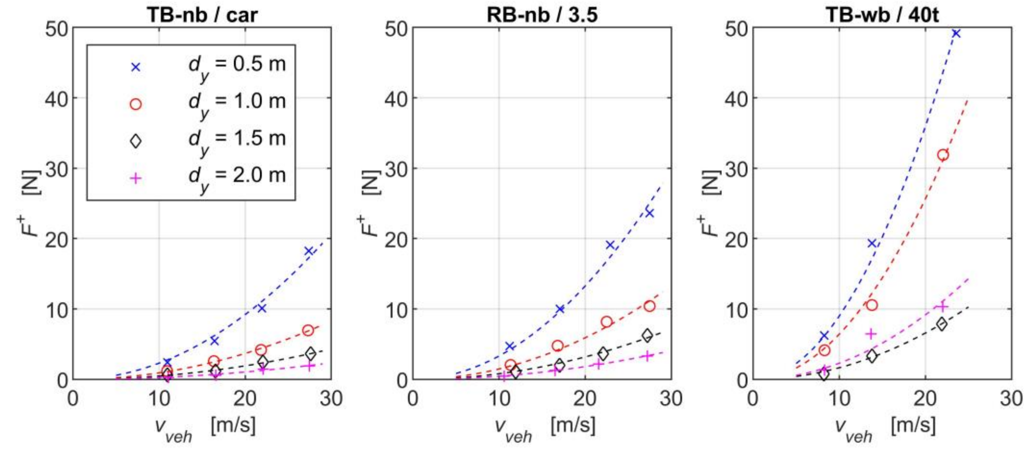

Fig. 3: Peak pressure load F^+ obtained for selected combinations of cyclist and vehicle types, see Fig. 1 for abbreviations (symbols: measurement data, dashed lines: curve fits accord. to Eq. (1)).

Fig. 4 shows c_1 versus overtaking distance d_y as established by curve fitting according to Eq. (1). Each panel presents c_1 values compiled for a specific cyclist type and differentiated according to vehicle type. The symbols indicate the established c_1 values and the lines show curve fits obtained with a power function relation according to

$$c_1 = c\, d_y^{\alpha}. \tag{2}$$

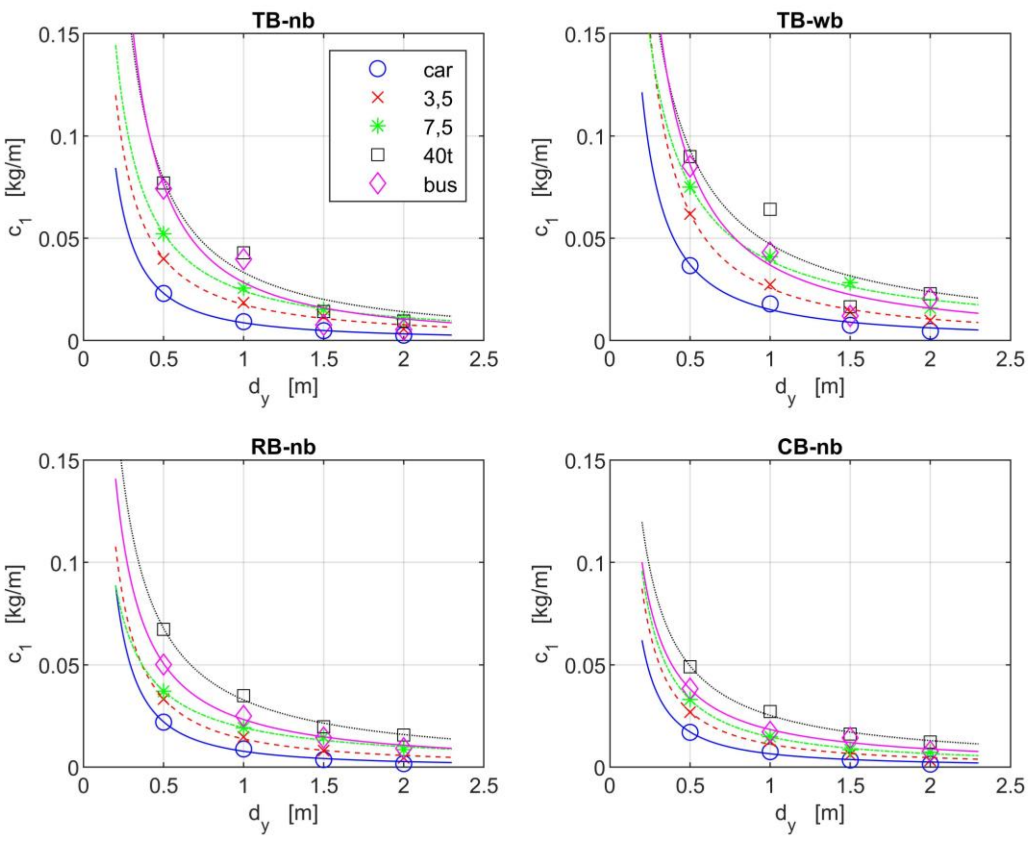

Fig. 4: Pre-factor c_1 for all cyclist types in dependency on vehicle type and overtaking distance d_y, see Fig. 1 for abbreviations (symbols: established values by curve fitting according to Eq. (1), lines: curve fits accord. to Eq. (2)).

This form of functional relationship between the pre-factor c_1 and overtaking distance d_y was inspired by the works of Sanz-Andrés et al. 2003, 2004a, 2004b, and Lichtneger and Ruck 2015, 2018 who studied transient aerodynamic loads induced by road and rail vehicles on various objects (traffic sign panels, pedestrians, pedestrian barriers, road-flanking walls). They established similar relations of this form and termed it 'distance model'.
The physical meaning of the exponent α in Eq. (2) is to describe how the disturbance originating from the overtaking vehicle spreads out with distance leading to the lateral load on the cyclist. Given the geometry boundary conditions with the street (ground) surface as a boundary plane which inhibits an unimpeded spreading of the disturbance, the values of the exponent are expected to lie between $-2 < \alpha < -1$. The physical meaning of the pre-factor c in Eq. (2) is less straightforward. In a general sense, it can be understood as a parameter which accounts for geometry related characteristics of the cyclist and the vehicle. In any case, it is desirable and target-aimed with regard to the development of a user-friendly model to relate both, the pre-factor c and the exponent α, to geometry characteristics of the cyclist and the vehicle.
The basic geometry parameters which determine the peak pressure load F^+ are the projected frontal area of the vehicle $A_{veh,fro}$ expressed by the product of the vehicle width W_{veh} and height H_{veh}, and the projected lateral area of the cyclist $A_{cyc,lat}$. It is acknowledged that next to these parameters also further geometry characteristics, such as e.g. the vehicle nose shape (cab over versus conventional cabin design), the ground clearance, or the distribution of the cyclist lateral area, to mention only a few, affect the peak pressure load. However, in the absence of quantitative descriptors for further possibly influencing factors, the evident assumption that the frontal and lateral areas are key parameters and other influencing factors are of minor relevance, and for the sake of developing a user-friendly model, an attempt was made to express the pre-factor c and exponent α as functions of vehicle width W_{veh}, height H_{veh}, and lateral cyclist area $A_{cyc,lat}$. To this end, the values for c and α as obtained by curve fitting according to Eq. (2) and pertaining to a specific cyclist type were displayed against products of power functions of H_{veh} and W_{veh} such that they can be described according to

$$c = m_c \left(H_{veh}^{c_H} \cdot W_{veh}^{c_W}\right) \tag{3}$$

and

$$\alpha = m_\alpha \left(H_{veh}^{\alpha_H} \cdot W_{veh}^{\alpha_W}\right). \tag{4}$$

Following systematic variations of the exponent pairs c_H with c_W and α_H with α_W and employing least square fits to the predicted and observed c and α values according to Eq. (3) + (4) and Eq. (2), respectively, resulted in exponent values $c_H = 1.4$ and $c_W = 0.0$, and $\alpha_H = -0.2$ and $\alpha_W = -0.3$ for all cyclist types. The corresponding pre-factors were $m_c = 4.8e\text{-}3$, 6.9e-3, 4.2e-3, 3.2e-3 and $m_\alpha = -1.97$, -1.79, -1.86, -1.83 for the adult cyclists on the touring bike without and with saddle bags, the adult cyclist on the racing bike, and the adolescent cyclist on the juvenile bike. Fig. 5 shows the observed pre-factor c and exponent α values (symbols) over abscissae with $H^{1.4} \cdot W^{0.0}$ and $H^{-0.2} \cdot W^{-0.3}$ scaling together with the predicted linear fits (dashed lines) according to Eq. (3) + (4) in the left and right column, respectively.

GALA e.V., Karlsruhe, Germany, ISBN 978-3-9816764-7-1

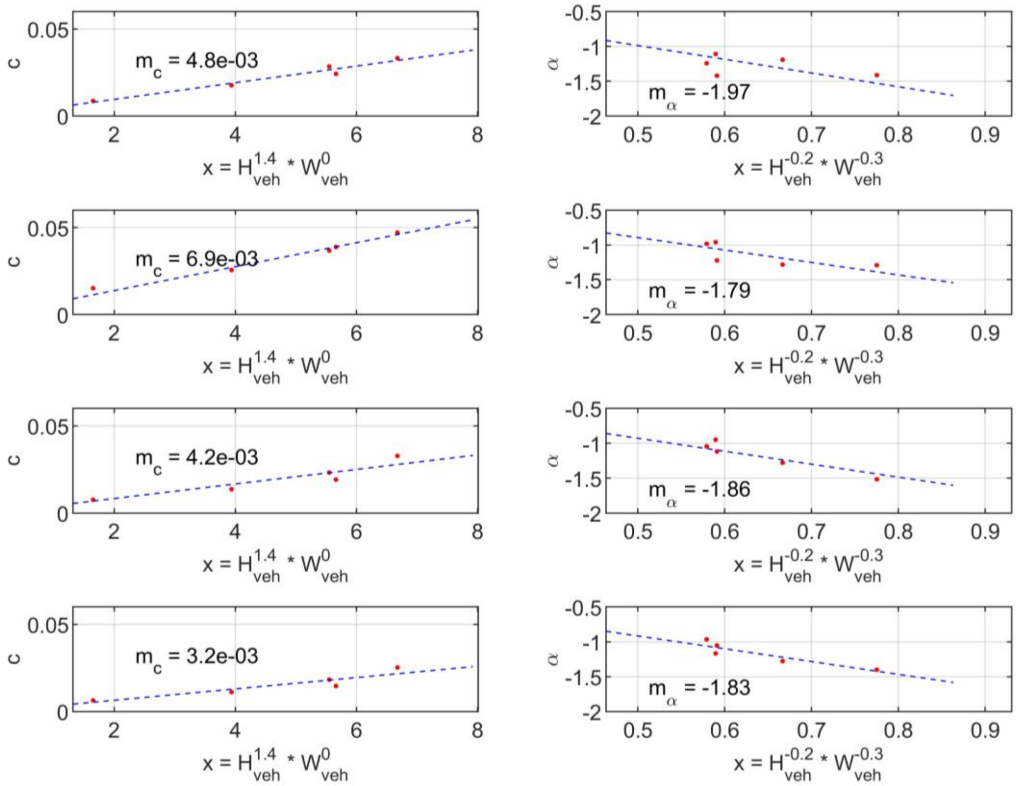

Fig. 5: Pre-factor c and exponent α as employed in Eq. (3) + (4) displayed over scaled abscissa $x = H_{veh}^{1.4}$ and $x = H_{veh}^{-0.2} * W_{veh}^{-0.3}$, respectively (symbols: established values by curve fitting according to Eq. (2), dashed lines: lines of best fits).

To further generalize the model, the pre-factors m_c and m_α have also to be related to basic geometry parameters of the vehicle and the cyclist. As can be seen by comparing the m_c values indicated in Fig. 5 and the cyclist lateral areas $A_{cyc,lat}$ indicated in Fig. 1, the order of m_c values is in line with the order of $A_{cyc,lat}$ values. This suggests a linear relation of the form

$$m_c = m_{c,pf}\ A_{cyc,lat}\ . \quad (5)$$

Based on a least square fit, the pre-factor $m_{c,pf}$ in Eq. (5) was determined to $m_{c,pf} = 0.0055$. The values of the pre-factor m_α do not exhibit a strong variation for the different cyclist types. Hence, for the sake of a user-friendly model, the pre-factor m_α is approximated by the mean over all cyclist types which is given by

$$\bar{m}_\alpha = \frac{1}{4} \sum m_\alpha = -1.86. \quad (6)$$

Combining Eqs. (1) to (6), a mathematical model for the peak pressure load F^+ can be established according to

$$F^+ = 0.0055 \cdot A_{cyc,lat} \cdot H_{veh}^{1.4} \cdot d_y^{-1.86 \left(H_{veh}^{-0.2} \cdot W_{veh}^{-0.3}\right)} \cdot V_{veh}^{2}. \quad (7)$$

The model-predicted peak pressure loads according to Eq. (7) are shown in Fig. 6 (dotted lines) together with the peak pressure loads obtained from the measurements (symbols) for the same selected combinations of cyclist-vehicle types as presented in Fig. 3. The comparison reveals an overall appropriate performance of the model.

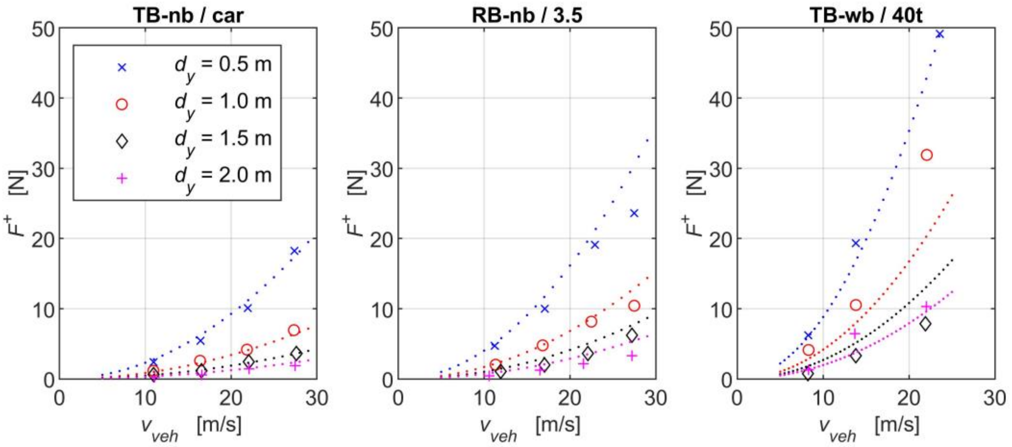

Fig. 6: Comparison of measured peak pressure load F^+ (symbols) obtained for selected combinations of cyclist and vehicle types with model predictions accord. to Eq. (7) (dotted lines), see Fig. 1 for abbreviations.

Peak suction load

The same approach as for the peak pressure load was also followed for the peak suction load F^-. The analogue exponents corresponding to Eq. (3) and Eq. (4) were determined to $c_H = 0.1$ and $c_W = 0.1$, and $\alpha_H = 0.0$ and $\alpha_W = -0.2$. The analogue pre-factors corresponding to Eq. (5) and Eq. (6) were evaluated as $m_{c,pf} = -0.0073$ and $\bar{m}_\alpha = -1.26$. Hence, the mathematical model for the peak suction load F^- reads as

$$F^- = -0.0073 \cdot A_{cyc,lat} \cdot H_{veh}^{0.1} \cdot W_{veh}^{0.1} \cdot d_y^{-1.26\left(W_{veh}^{-0.2}\right)} \cdot V_{veh}^{2}. \qquad (8)$$

The model-predicted peak suction loads according to Eq. (8) are shown in Fig. 7 (dotted lines) together with the peak suction loads obtained from the measurements (symbols) for the same selected combinations of cyclist-vehicle types as presented before. Compared to the model-predicted peak pressure loads, the performance appears somewhat lower. However, given the fact that the magnitudes of the peak suction load F^- are multiple times smaller than those of the peak pressure load F^+, the overall model performance is considered to be adequate.

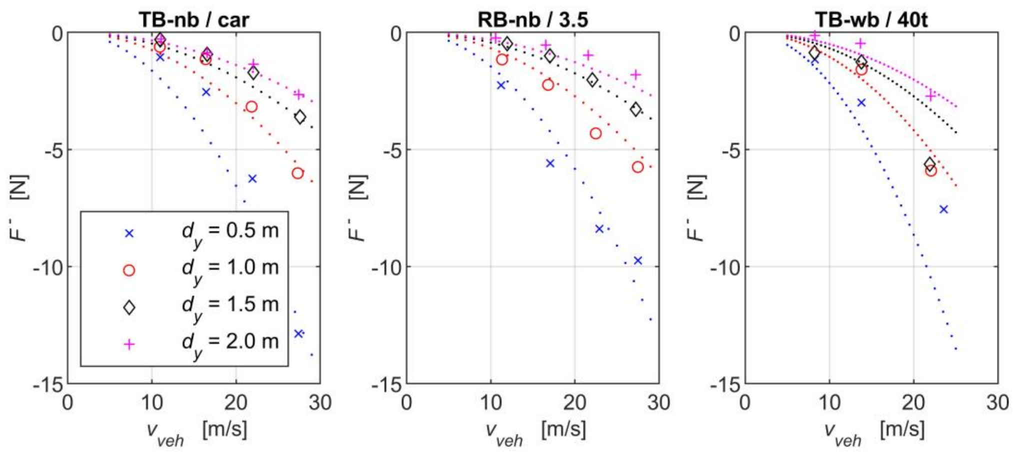

Fig. 7: Comparison of measured peak suction load F^- (symbols) obtained for selected combinations of cyclist and vehicle types with model predictions accord. to Eq. (8) (dotted lines), see Fig. 1 for abbreviations.

Flip over load

Based on the models for the peak pressure load (Eq. 7) and for the peak suction load (Eq. 8), the total change from pressure to suction load which a cyclist experiences within a very short time span when overtaken by a vehicle can be estimated. The sum of the absolute loads is termed flip over load F_{fo} as it occurs relatively sudden and rapid and can be determined according to

$$F_{fo} = |F^+| + |F^-| \tag{9}$$

with F^+ and F^- according to Eq. (7) and Eq. (8), respectively.

Summary and Conclusions

A mathematical model to calculate the aerodynamic peak lateral loads of pressure and suction which act on a cyclist when being overtaken by a vehicle was developed. The model can be applied for various cyclist types (adult person on touring bike with / without saddle bags, adult person on racing bike, adolescent person on juvenile bike) and various vehicle types (station wagon, 3.5 t van, 7.5 t truck, 40 t semitrailer truck, tour bus). The model covers peak pressure and suction loads for a wide range of overtaking maneuver conditions in terms of overtaking distance and speed. Furthermore, based on the peak pressure and suction load, the so termed flip over load can be determined. The flip over load characterizes the sudden and rapid change in the direction of the lateral load from pressure to suction as experienced by a cyclist during an overtaking maneuver and is considered to establish a meaningful quantity to assess cyclist safety.

Acknowledgements

The authors gratefully acknowledge the financial support of the Deutsche Forschungsgemeinschaft DFG (German Research Foundation) under grant Ru 345/32-3.

References

Gromke, C., Ruck, B., 2019a: Aerodynamic loads on a cyclist while overtaking by a vehicle. Proc. 27. GALA Fachtagung "Experimentelle Strömungsmechanik", Erlangen, Germany, Sep. 2019, pp. 7.1–7.8

Gromke, C., Ruck, B., 2019b: Aerodynamic loads on a cyclist passed by a passenger car. Proc. 15th International Conference on Wind Engineering ICWE15, Beijing, China, Sep. 2019, 4 p

Gromke, C., Ruck, B., 2021: Passenger car-induced lateral aerodynamic loads on cyclists during overtaking. J. Wind Eng. Ind. Aerodyn. 209:104489, 13 pp

Lichtneger, P., Ruck, B., 2015: Full scale experiments on vehicle induced transient loads on road-side plates. J. Wind Eng. Ind. Aerodyn. 136:73–81

Lichtneger, P., Ruck, B., 2018: Full scale experiments on vehicle induced transient pressure loads on roadside walls. J. Wind Eng. Ind. Aerodyn. 174:451–457

Sanz-Andrés, A., Santiago-Prowald, J., Baker, C., Quinn, A., 2003: Vehicle-induced loads on traffic sign panels. J. Wind Eng. Ind. Aerodyn. 91:925–942

Sanz-Andrés, A., Laverón, A., Cuerva, A., Baker, C., 2004a: Vehicle-induced force on pedestrians. J. Wind Eng. Ind. Aerodyn. 92:185–198

Sanz-Andrés, A., Laverón, A., Baker, C., Quinn, A., 2004b: Vehicle induced loads on pedestrian barriers. J. Wind Eng. Ind. Aerodyn. 92:413–426